NeuroImage 112 (2015) 61–69

Contents lists available at ScienceDirect

NeuroImage

journal homepage: www.elsevier.com/locate/ynimg

Gestalt perception is associated with reduced parietal beta oscillations

Natalia Zaretskaya *, Andreas Bartels *

Centre for Integrative Neuroscience, University of Tübingen, Tübingen, Germany

ARTICLE INFO

Article history:
Accepted 23 February 2015
Available online 27 February 2015

Keywords:
Attention
EEG
Oscillations
Gestalt
Parietal cortex

ABSTRACT

The ability to perceive composite objects as a whole is fundamental for visual perception in a complex and cluttered natural environment. This ability may be mediated by increased communication between neural representations of distinct object elements, and has been linked to increased synchronization of oscillatory brain activity in the gamma band. Previous studies of perceptual grouping either guided attention between local and global aspects of a given stimulus or manipulated its physical properties to achieve grouped and ungrouped perceptual conditions. In contrast to those studies, we fully matched the physical properties underlying global and local percepts using a bistable stimulus that causes the viewer to perceive either local motion of multiple elements or global motion of two illusory shapes without any external change. To test the synchronization hypothesis we recorded brain activity with EEG, while human participants viewed the stimulus and reported changes in their perception. In contrast to previous findings we show that power of the beta-band was lower during perception of global Gestalt than during that of local elements. Source localization places these differences in the posterior parietal cortex, overlapping with a site previously associated with both attention and Gestalt perception. These findings reveal a role of parietal beta-band activity in internally, rather than externally or attention-driven processes of Gestalt perception. They also add to the growing evidence for shared neural substrates of attention and Gestalt perception, both being linked to parietal cortex.

Introduction

The ability to group local elements into a whole is one of the cornerstones of visual perception. It allows us to infer object shapes during partial occlusion and to make sense of complex scenes. The loss of this ability due to brain lesion or neurodegeneration can severely hinder patients' everyday lives (Balint, 1909; Kirshner and Lavin, 2006; Luria, 1959; Wolpert, 1924).

Selective increase in communication between neuronal populations representing the object elements, which may manifest itself through synchronization of oscillatory activity, has been proposed as a potential mechanism of perceptual grouping (Fries, 2005; Singer, 2007; Tallon-Baudry, 2009). The synchronization may occur locally within the same area or involve long-range projections between higher and lower- level areas (Fries, 2005). The local synchronization will be reflected in an amplitude increase of intracortically measured local field potentials or scalp EEG, while long-range synchronization would show up as an increase in oscillatory phase coupling between signals in two areas. Indeed, multiple studies point to the importance of a transient increase in gamma band power and coherence for global perception of hierarchical stimuli as well as for interhemispheric integration and illusory contour perception (Rose and Büchel, 2005; Rose et al., 2006; Strüber et al., 2013; Tallon-Baudry et al., 1996). In addition, there is accumulating evidence for the role of theta and beta phase synchrony in grouping and illusion perception, which may be mediating information exchange between higher and lower level areas (Hanslmayr et al., 2013; Hipp et al., 2011; Keil et al., 2014; Romei et al., 2011; Smith et al., 2006; Volberg et al., 2013).

Most previous studies examining oscillatory correlates of perceptual grouping either guided attention between local and global stimulus features (Rose et al., 2006) or physically manipulated the stimulus to enhance global or local aspects (Aissani et al., 2014; Romei et al., 2011; Smith et al., 2006; Tallon-Baudry et al., 1996). This turned them either into studies of directed attention (Sasaki et al., 2001) or introduced physical confounds that could explain differences in neural activity. In addition, prior studies only analysed the brief time epochs around the stimulus onset in order to examine neural correlates of Gestalt formation. However, this approach left neural correlates involved in sustaining continuous Gestalt perception unexplored.

Here we circumvented these limitations by using a bi-stable stimulus that leads perception to alternate spontaneously between a local, ungrouped percept and global Gestalt. This avoided changes in physical properties and instructed shifts of attention (Anstis and Kim, 2011; Zaretskaya et al., 2013) (Fig. 1). We recorded EEG while human participants viewed the stimulus and reported spontaneous changes in their perception. The entirely spontaneously occurring perceptual alternations allowed us to study both, transitions between local and global

* Corresponding authors at: Vision and Cognition Lab, Centre for Integrative Neuroscience, University of Tübingen, Otfried-Müller-Str. 25, 72076 Tübingen, Germany.
E-mail addresses: natalia.zaretskaya@tuebingen.mpg.de (N. Zaretskaya), andreas.bartels@tuebingen.mpg.de (A. Bartels).

http://dx.doi.org/10.1016/j.neuroimage.2015.02.049
1053-8119/

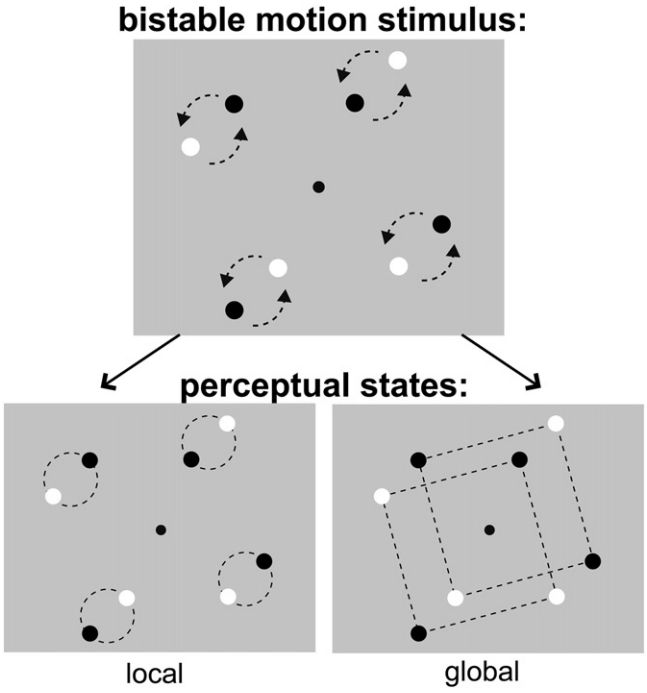

Fig. 1. Bistable stimulus that induced spontaneously alternating perceptual states of either local element motion or global Gestalt motion. Top: four dot pairs, consisting of a white and a black dot each, moved on circular trajectories indicated by dotted arrows. Bottom: the stimulus can be perceived as four local dot pairs or as global Gestalt consisting of two large squares (indicated by dotted lines).

percepts as well as continuous Gestalt perception, without physical or attentional confounds. Oscillatory EEG signal of different frequency bands was analyzed to examine local synchrony as well as long-range phase-coupling changes as a function of the subjective percept. Analyses were carried out both in electrode space and in source space using two different source localization techniques.

Materials and methods

Participants

A total of 24 healthy right-handed participants (age range 18–46, 11 females, 1 author) took part in this study. All had normal or corrected-to-normal vision and gave written informed consent prior to participation. The study was conducted according to the Declaration of Helsinki and was approved by the ethics committee of the University Clinic Tübingen.

Stimuli and task

Participants were seated in a comfortable chair with their head on a chin rest. The stimulus was generated using Cogent 1.29 (John Romaya, Wellcome Department of Imaging Neuroscience, University College London) on a Windows PC running MATLAB 2010a (MathWorks, Inc., Natick, USA) and presented via a linearized monitor (Samsung SyncMaster 2443). The monitor had a resolution of 1920x1200 pixels and a 60 Hz refresh rate, and was placed at a viewing distance of 54 cm.

The stimulus consisted of four white and four black dots. Because the stimulus perception is typically dominated by the global interpretation (Anstis and Kim, 2011; Zaretskaya et al., 2013), we assigned luminance to each dot in a way which was inconsistent with the group to which it belongs (Fig. 1). This was previously shown to decrease the probability of seeing the global percept (Anstis and Kim, 2011). The stimulus spanned 8 degrees of the visual angle along the diagonal. Each individual dot had a size of 0.5 degrees. The distance between two neighboring dots was 1 degree, and the distance between each dot pair was 5.66 degrees. On each stimulus presentation, the whole stimulus sheet was tilted by either + 15 or − 15 degrees to prevent local adaptation effects.

Procedure

The experimental procedure consisted of the following steps. First, the electrodes were placed and impedances below 10 kOhm were achieved. Impedances were kept below this value throughout the whole experiment. After electrode placement participants were familiarized with the task and performed 1–3 test runs comprising 2 trials each. During the test trials, the speed of the dot rotation was adjusted to maximally match the duration of global and local percepts (according to our unpublished observation, higher speed reduces the duration of the global percept). After this, the speed of the dot rotation was kept constant throughout the experiment. The resulting average rotation speed was 2.5 ± 0.23 cycles per second (mean ± SD across subjects).

The experiment consisted of 8 runs, each lasting 8 minutes. Each run contained 8 continuous viewing trials. Subjects were instructed to fixate throughout each trial. Trials started with a two second baseline period, followed by 45 seconds of stimulus presentation. During stimulus presentation they were also required to report changes in their perception from global to local and from local to global by pressing the two corresponding buttons with two fingers of their right hand. They were explicitly instructed not to enforce either of the percepts voluntarily. Each trial ended with thirteen seconds of rest, which was indicated by a green fixation dot. During these periods subjects could rest their eyes and look freely on the screen.

EEG data acquisition

EEG was recorded using a 64-channel actiCAP with Ag/AgCl electrodes, two BrainAmp MR plus amplifiers (bandpass 0.016–250 Hz) and Vision Recorder software (Brain Products, Inc., Munich, Germany), and digitalized at a sampling rate of 500 Hz. The electrode positions followed an international 10–20 system and were referenced against FCz. A single EOG channel was placed below the left orbit.

EEG data analysis

EEG data were analyzed with MATLAB 2012b (MathWorks, Inc., Natick, MA, USA), the open source FieldTrip toolbox (http://www.ru.nl/fcdonders/fieldtrip) and custom scripts.

Preprocessing

The preprocessing of EEG data consisted of the following steps. First, raw data were epoched into 47-second trials. Each trial comprised 2 seconds of baseline and 45 seconds of stimulus presentation. The resulting time segments were examined for eye blinks, muscle and other artifacts. Time segments containing these artifacts were removed from the data. Following this, in order to eliminate more subtle artifacts like small eye movements and muscle twitches, the gross cleaned data were concatenated and subjected to independent component analysis (Jung et al., 2000). Components representing artifacts were identified by careful visual inspection of their time course and scalp topography, and eliminated from the data. An average of 22.83 ± 8.49 components were removed (mean across subjects ± SD). After this, data from 63 EEG channels were notch-filtered at 50, 100 and 150 Hz and referenced against the average. For source localization using sLORETA they were additionally band-pass filtered at 1–45 Hz prior to rereferencing.

Epoch definition

After preprocessing we defined epochs of global and local perception. In our main analysis we intentionally focused on Gestalt *perception* rather than the process of Gestalt *formation*. This allowed us to avoid brain activity related to motor response and decision-making close to

perceptual switches. To achieve this, we defined global and local epochs as follows. First, percepts that lasted at least three seconds were selected based on button responses. From each of these percepts, the central one-second of data was taken as an epoch. As a result, the onset and the offset of each epoch was at least one second away from any button press. The number of global and local epochs of each subject was equated by randomly sampling trials from the condition with the larger number of epochs. Defining one-second long segments and equating the number of segments allowed us to avoid any statistical bias induced by differences in the sample size. This procedure resulted in 108.96 ± 31.74 epochs (mean ± SD; range: 54–175) per participant for each condition. Additionally, artifact-free 'baseline' epochs were defined as one second directly preceding the stimulus onset (46.00 ± 11.89 epochs per participant). This epoching procedure is illustrated in Fig. 2 (top). The baseline epochs were subsequently used to normalize global and local power spectra for statistical analysis and for illustration of stimulus effects relative to baseline. They were not used for statistical comparisons with the other two conditions.

Although our main analysis focused on periods of stability we also examined oscillatory activity around the time when subjects reported perceptual changes. We did this to be able to compare our results with a recent study by (Flevaris et al., 2013) that reported an alpha-band decrease before the onset of the global percept using a similar experimental paradigm with a bistable diamond stimulus. We defined segments of data 1.5 seconds before and 1.5 seconds after each button press that were free of eye blinks, other button presses, or other artifacts. The procedure resulted in 81.43 ± 52.77 (mean ± SD, range: 5–185) periswitch epochs per subject. One subject had to be excluded because no epochs could be identified that would satisfy our criteria in both conditions. Because of the small number of trials compared to our main analysis and presumably lower statistical power, we did not perform source localization analyses for this part and report only results in electrode space.

Sensor-level power analysis

For the main analysis spectral power at each frequency was derived from a fast Fourier transform using the multitaper method. To achieve optimal estimates of power at low (5–30 Hz) and high (31–120 Hz) frequencies we analyzed them separately. The power at lower frequencies was estimated for each discrete frequency using a single (Hanning) taper. For estimating the high-frequency power we used discrete prolate spheroidal (slepian) sequences (DPSS) with a frequency smoothing of ± 8 Hz. The power of neural oscillations at different frequencies is approximately inversely related to the frequency (Buzsáki and Draguhn, 2004). Therefore, for better visualization and cluster-level statistics in the frequency domain we normalized the power spectra to baseline by computing the relative power change (e.g. (global-baseline)/baseline) for each electrode and each frequency. Note that our experimental design did not allow us to normalize every epoch by its unique preceding baseline as is typically done in MEG and EEG studies. Therefore we normalized the trial-averaged power of global and local conditions by the average power during the baseline in each subject.

To access differences in relative power change between local and global conditions we employed statistical non-parametric mapping and cluster-level inference (Maris and Oostenveld, 2007; Nichols and Holmes, 2002). First, a paired-sample non-parametric randomization test with 10000 randomizations using Monte Carlo bootstrapping approximation was done for each point in a two-dimensional electrode-frequency space using t-statistic. To control for type I error due to multiple comparisons, clusters of points in this two-dimensional space exceeding a significance level of $p \leq 0.05$ (two-tailed test) were determined, and an integral of t-values in a cluster was used as a cluster-levels statistic. The statistical significance of each cluster was determined in a second randomization test with 10000 randomizations. A cluster was considered significant at $p \leq 0.05$ (two-tailed test). This statistical analysis was performed separately for higher and lower frequencies. Unless stated otherwise, we employed the same statistical analysis for all of the following group-level statistics in this study.

For the significant frequency bands identified in the analysis described above, and in order to compare our results with those of (Flevaris et al., 2013) we also performed an additional time-resolved power analysis of the 3-second time intervals around the reported perceptual transitions using wavelet analysis in the frequency domain. We estimated power separately for the alpha (8–12 Hz identified by Flevaris et al.) and the beta (13–23 Hz identified in this study) band using DPSS. The length of the time window was set for each frequency separately to include seven oscillatory cycles, and was centered on 121 time points ranging from −1.5 to 1.5 relative to the button press. We then searched for the time points that showed a significant difference between the transition from local to global versus global to local percepts using a non-parametric statistical procedure with cluster-level inference.

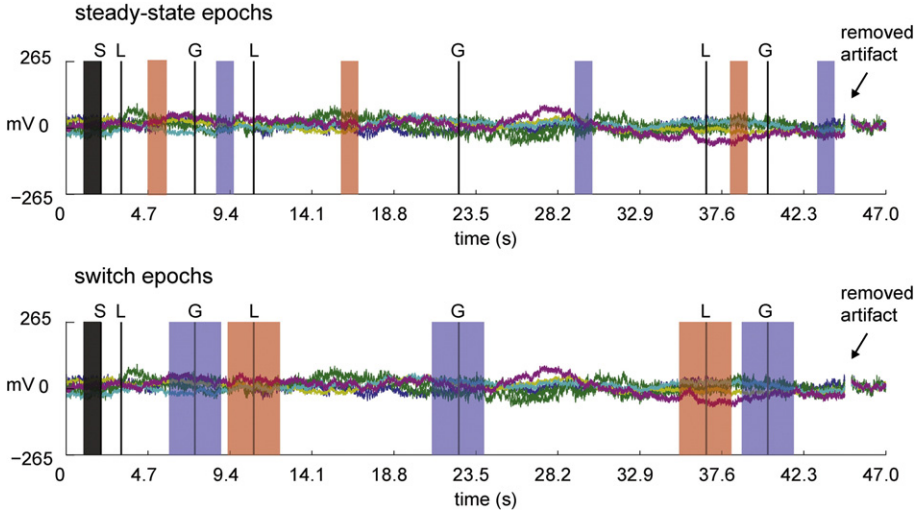

Fig. 2. Illustration of epoch definition for baseline, global and local percepts within a given 47 s trial. Vertical black lines with letters on top illustrate the onsets of stimulus ("S") as well as button presses signaling onsets of global ("G") and local ("L") percepts. Baseline epochs (black bars preceding "S") were defined as an artifact-free one-second data segment before the stimulus onset. Top: global and local steady-state epochs (light purple and red bars, respectively) were defined as artifact-free one second of data located equally far away (at least one second) from any button press. This procedure was used to minimize decision and motor-related activity in the data. Bottom: transition epochs (light colored bars) were defined as artifact-free segments extending 1.5 s before and 1.5 s after each button press.

Localizing cortical sources of band-limited power differences

After having determined that beta-band power in the range 13–24 Hz decreases significantly in global compared to local perceptual states, we localized the cortical generators of this power difference. Please note that the approach of first identifying the relevant frequencies in the electrode space, and then localizing its cortical generators is not circular. Circularity in statistical analysis (a problem known in fMRI as "double-dipping") is produced when the first step involves data selected for hypothesis testing that is not independent from the actual hypothesis test at the second step. Here, in contrast, the first step already constitutes an actual hypothesis test about *what* frequencies are different in the two conditions. This test is done with appropriate multiple comparison correction and without prior data selection (whole available frequency spectrum is investigated). After that, we do a second, different hypothesis test about *where* this difference is generated, which is a common practice in EEG and MEG research (see also Gross et al., 2013 p.361).

Also note that the frequency range that showed a significant difference in our assumption-free analysis corresponds exactly to the conventional beta-band (Niedermeyer and Lopes da Silva, 2005), so our result would have been exactly the same had we defined the beta-band independent of the data based on the literature.

To localize sources of beta-band differences in power we used two independent source localization approaches: standardized low-resolution electromagnetic tomography (sLORETA) (Pascual-Marqui, 2002) and adaptive linear spatial filtering ("beamforming") (Gross et al., 2001). The forward model in both cases was identical. It consisted of 6239 cortical locations (spaced at 5 mm distance) derived from a standard MNI volume (MNI152) and a boundary-element head model of the same volume.

sLORETA belongs to a family of minimum norm distributed source solutions which attempt to find the distribution of source activity that best explains the observed scalp topography. It assumes smooth distribution of source values along the cortical surface, and therefore produces low-resolution maps. sLORETA can provide an estimate of the current source density power at the cortical surface, and has been previously used to localize oscillatory activity in EEG data (Olbrich et al., 2009; Pascual-Marqui et al., 2002). We used the sLORETA implementation from the author's website (http://www.uzh.ch/keyinst/loreta.htm). Preprocessed one-second EEG epochs were imported into the software, where sensor-level cross-spectra for each condition were computed in the frequency range of interest. These cross-spectra were then transformed into source space, yielding an estimate of beta-band power at each voxel and each condition. These source-space data were imported back into MATLAB/FieldTrip for statistical comparison. To determine differences between global and local conditions, raw power values were subjected to a paired-sample non-parametric test with cluster-level inference, which was identical to the sensor-level procedure.

To provide additional independent evidence for the location of beta-band differences in the brain, we also used adaptive linear spatial filtering ("beamforming"). In beamforming a spatial filter is constructed at each cortical location, which passes activity from that location while maximally suppressing activity from all other locations. The major advantage of beamforming is that it estimates the contribution of each source location independently rather than trying to fit a source distribution that best explains the scalp topography. It is therefore less likely to produce false positive results. However, beamforming is known to be less sensitive in detecting correlated sources (Van Veen et al., 1997). We used the DICS (dynamic imaging of coherent sources) beamformer implementation in FieldTrip to construct a common spatial filter based on combined data from global and local conditions. The procedure consisted of the following steps. First complex Fourier spectra were computed for the frequency band of interest (13–24 Hz) from the sensor-level data using the multitaper method. The sensor-level cross-spectral densities were computed from the complex spectra by multiplying them with their complex conjugate. After this, the cross-spectrum was used to derive beta-band power at each cortical location by multiplying it with the corresponding spatial filter for that location. The statistical comparison of power in global and local conditions was identical to that of sLORETA.

Sensor-level phase coupling analysis

To quantify changes in phase coupling between higher and lower areas and/or across hemispheres for global and local perceptual states we calculated the imaginary part of coherency (Nolte et al., 2004). The imaginary part of coherency allows assessing consistent phase offsets between two signals across trials, while discarding zero and 180° phase offsets, which are thought to arise in sensor space through volume conduction. In brief, for each pair of electrodes we first computed their individual complex Fourier spectra for every trial using the same procedure as described above for sensor-level power analysis (one second segments, 63 electrodes, 26 low and 90 high frequencies). Complex spectra were used to compute cross-spectral densities between all channel pairs by multiplying the spectra with their complex conjugates. Coherency was computed in its complex form by normalizing the cross spectral density by the product of individual autospectral densities. After this, instead of using the magnitude and phase of coherency as a measure of coupling, the imaginary part of coherency was used for statistical analysis. If the phase offset between two signals is random, the imaginary part of coherency approaches zero. If, in turn, a systematic phase offset exists between the two, the imaginary part becomes either positive or a negative depending on whether the first signal lead or lags the second one.

Using this analysis for every subject and every condition we obtained a three-dimensional matrix of phase coupling measures ($63 \times 63 \times 26$ for low frequencies, $63 \times 63 \times 90$ for high frequencies). To compare changes in coupling between global and local conditions, we performed a non-parametric paired randomization test with cluster-level inference.

Source-level phase coupling analysis

To achieve maximum sensitivity in our source analysis and to avoid explosion in the number of statistical comparisons we took a hypothesis-driven approach about the frequency bands that could exhibit differential coupling between conditions in the source space. We focused on the three frequency bands of interest, for which oscillatory phase synchronization has been reported previously, namely theta, beta and gamma bands. Although we are not aware of any reports on alpha-band phase synchrony related to perceptual grouping, we also added the alpha band for completeness. We used the standard definitions of theta, alpha and beta bands, namely 4–7 Hz for theta, 8–12 Hz for alpha, and 13–24 Hz for the beta band (Niedermeyer and Lopes da Silva, 2005). The lower gamma (35–45 Hz) band was defined based on the findings of Rose and Büchel, 2005 and Rose et al., 2006.

Based on our previous fMRI and TMS results (Zaretskaya et al., 2013), we hypothesized that the right PPC may play a key role in perceptual grouping through long-range phase synchronization with other areas. We therefore defined the right PPC as the reference source using the coordinates from the peak activation in the contrast "global versus local" (MNI coordinates $x = 34$, $y = -40$, $z = 52$, see Results) from our previous fMRI study. To identify areas that were differentially phase-coupled to the right PPC in global and local conditions, we performed a whole-brain coherence analysis using the DICS beamforming procedure separately for each frequency band of interest. Sensor-level cross-spectral densities were used to derive source-level cross-spectral densities between the right PPC and every other voxel by linear spatial filtering using a common filter created from global and local conditions. Since source-level signals are less affected by volume conduction we computed conventional coherence magnitude, rather than the imaginary part of coherency, between the right PPC and every other voxel. To compare source-level coherence maps we

z-transformed the values and performed a voxel-wise non-parametric randomization test with cluster-level inference.

In addition, we also performed a region of interest analysis for the areas that we know to play a role in stimulus processing (Zaretskaya et al., 2013): left and right PPC, left and right extrastriate areas (putative V5/MT+) and early visual cortex. Our early visual cortex ROI was centered on the occipital pole (MNI coordinates: x = 0, y = −100, z = 0). The coordinates of extrastriate cortex (putative V5/MT+) and the PPC were taken from our previous fMRI study for the contrast "stimulus > baseline" at $p < 0.05$ uncorrected (left ESC x = −50 y = −74 z = 00; right ESC x = 46 y = −68 z = −02; left PPC x = −36 y = −58 z = 66; right PPC x = 28 y = −56 z = 54). All regions of interest consisted of voxels within a radius of 10 mm from the above coordinates. For the region of interest analysis we employed small volume correction for multiple comparisons (i.e. only taking into account voxels within a ROI). It was performed with non-parametric randomization test using the maximum value statistic.

Results

Behavior

We recorded EEG activity while subjects viewed the bistable stimulus and reported their global and local perceptual states (Fig. 1). The average global and local percept durations during the experiment across subjects were 7.64 ± 2.80 and 5.72 ± 2.63 seconds (mean ± SD) respectively (see also Supplemental Fig. S1 for histograms of the durations of each percept type). The EEG epochs that were used for analysis (see "Epoch definition" above) were taken from global and local percepts with an average duration of 4.52 ± 1.36 and 3.83 ± 1.37 seconds (mean ± SD) respectively. The average percept periods from which the one-second epochs were defined did not differ significantly in duration (paired t-test, p = 0.06, t(23) = 1.99).

EEG power

First we examined the differences in signal power associated with global and local perception at the sensor level (i.e. at every electrode). We focused our analysis on the continuous, steady state part of perception in the middle of the perceptual period, at least one second away from any perceptual transition (see Fig. 2). To achieve better accuracy we analyzed low (1–30 Hz) and high (31–120 Hz) frequency bands separately (see methods for details). Fig. 3A shows that perception of global Gestalt compared to perception of local components was associated with a significant decrease in power of frequencies covering the beta band (13–24 Hz) (Fig. 3, cluster statistic = −640, p = 0.002). This difference in beta power is unlikely to have resulted from the slight predominance of the global percept in the behavioral data (see above), as the mean differences in overall percept durations and the differences in beta-band power between global and local percepts were uncorrelated across subjects (Pearson's r = −0.11, p = 0.62).

We also ruled out that this difference is due to an interaction between percept order (when participants view the stimulus, the first percept is typically a local one, followed by the global (Anstis and Kim, 2011)) and a potential steady decrease of beta-band power over time. We correlated beta power in each analyzed percept with the time point within a trial when that percept occurred. The average correlation coefficient across subject was 0.021 ± 0.104 (SD), and it was not significantly different from zero (one-sample two-tailed t-test with Fisher-transformed correlation coefficients t(23) = 1.96, p = 0.062). Note that the trend here is towards the positive correlation, which completely contradicts this alternative explanation.

We did not find any significant power change for the high frequencies in our data (absolute cluster statistic ≤390, p ≥ 0.076, trend towards negative values, i.e. local > global). Since gamma, especially in the higher frequencies is difficult to detect with EEG, we tested whether

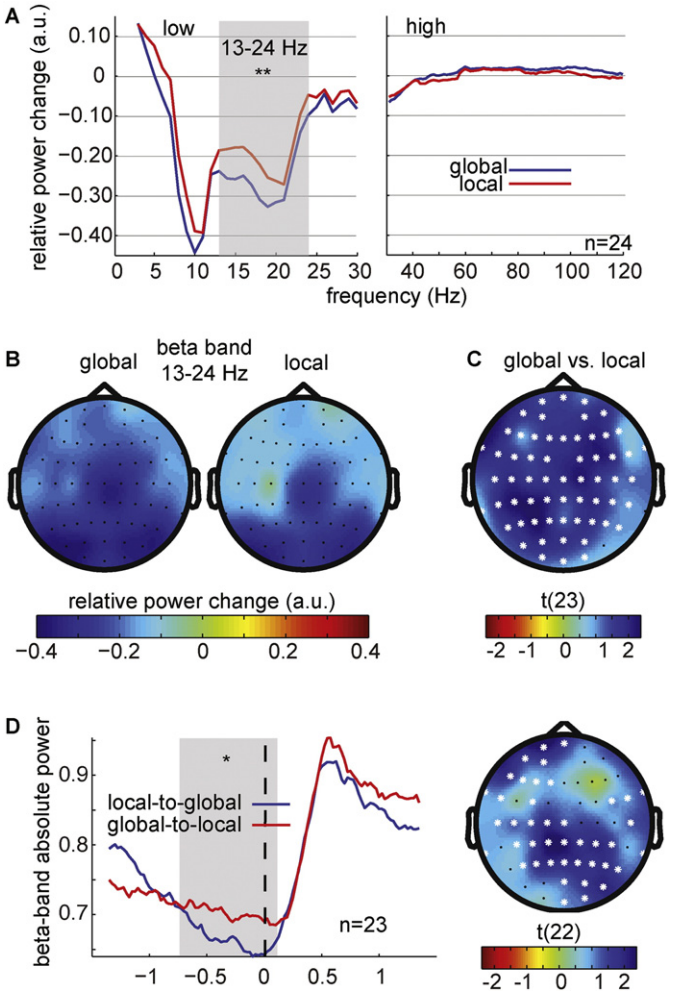

Fig. 3. Results of the spectral analysis in sensor space. (A) Mean relative power change in global and local conditions relative to baseline (average across all electrodes). The power was estimated separately within two frequency bands, 5–30 Hz and 31–120 Hz (see Materials and Methods for details). The grey area illustrates the frequency range contributing to the significant difference between global and local conditions. Power decreased in a broad frequency range from alpha to low gamma, but only beta band (13–24 Hz) differed significantly between conditions. (B) Topographic distribution of the beta-band decrease (average over twelve discrete frequencies from 13–24 Hz) across the scalp for global and local conditions. The decrease is most prominent at posterior and central electrodes. (C) Topographic distribution of the t-statistic comparing global and local conditions. Electrodes that contributed to the significant cluster at least in one of the discrete frequencies between 13 and 24 Hz are indicated by white dots. (D) Beta-band power changes around the perceptual switch, averaged across all electrodes. The grey bar indicates a significant cluster across electrodes and time, derived from comparing beta power between global and local conditions. The channels contributing to this cluster were mostly located in the frontal and parietal regions.

we can detect any stimulus-induced signal in the gamma band. We first defined artifact-free epochs of ± one second around the stimulus onset. We then analyzed frequency power in the one-second interval before the stimulus and after the stimulus onset using analysis parameters that were identical to our main analysis (DPSS taper with 8 Hz smoothing, all individual frequencies from 31 to 120 Hz). We then statistically compared one-second epochs immediately preceding and one-second epochs immediately following the onset of visual stimulation. Despite the low number of artifact-free epochs per subject (40.96 + −13.40) we did find a significant decrease during the stimulus onset compared to its preceding baseline (cluster statistic = −3894, p = 0.001) in the lower gamma range between 31 and 65 Hz, peaking in at the occipital electrode Oz. This finding suggests that in principle we were able to detect signals in the lower gamma band, but that there was no difference between global and local perceptual states in this band. Nevertheless we

acknowledge that discovery of eye movement artifacts in the gamma band for MEG/EEG data (Yuval-Greenberg et al., 2008) as well as generally low sensitivity of EEG to gamma does not allow us to make a confident statement about the absence of gamma activity in this study.

Given the decrease in beta-band power during continuous perception of global Gestalt, we wanted to test whether and at which time intervals this decrease would be detectable around the time of the perceptual switch. We therefore additionally calculated the temporal evolution of the beta-band power around the switch from local to global and from global to local perceptual states. We found a significant (cluster-level statistic $= -877$, $p = 0.03$) decrease in the beta-band starting around 0.7 seconds before and ending at 0.1 seconds after the onset of the global percept compared to that of the local percept (Fig. 3D). The channels contributing to this cluster were mostly located in the frontal and parietal regions.

We did not find any significant change in alpha power (8–12 Hz), neither for the whole time range (cluster-level $p \geq 0.46$, absolute cluster statistic ≤ 41.51), nor for the average signal within the time window of -0.5 to -0.1 seconds as reported by Flevaris et al. (2013) who used a similar experimental paradigm (all $p \geq 0.07$ uncorrected, absolute $t \leq 1.50$).

Source localization of beta-band power decrease

As the sensor-level analysis showed that beta-band (13–24 Hz) power differed between global and local perceptual states, we further performed source localization analysis to identify the cortical generators of these differences. Source localization of EEG and MEG data does not have a unique and optimal solution. Therefore, to be able to make stronger claims about the location of the differences, we used two independent source localization approaches: standardized low-resolution electromagnetic tomography (Pascual-Marqui, 2002) and adaptive linear spatial filtering (Gross et al., 2001).

Comparing the beta-band power in global and local conditions estimated with sLORETA yielded a significant negative cluster (825 voxels, $p = 0.026$) covering bilateral parietal cortices with a peak at the left superior parietal lobe (Fig. 4A (left), MNI coordinates: left: $x = -12$, $y = -64$, $z = 60$; right: $x = 24$, $y = -62$, $z = 56$, BA7).

The statistical comparison using power estimates derived from beamforming also yielded a significant negative cluster, which included 85% of all voxels (5305 voxels, cluster-level $p = 0.002$). Its peak was also located in the posterior parietal cortex, but in the right hemisphere (Fig. 4A (right), MNI coordinates $x = 10$, $y = -52$, $z = 66$, BA5/BA7). When mirrored onto the same hemisphere, the peaks identified with each of the methods were only 13 mm apart. Thus, although the peaks of the two source localization methods were in different hemispheres, both of them localized beta band decrease to a similar location in posterior parietal cortex.

Phase coupling sensor-level results

In addition to investigating local synchronization differences reflected in power changes we wanted to determine whether global and local perceptual states were accompanied by differential long-range phase coupling between higher and lower areas and/or across hemispheres, as it has been suggested by prior experimental findings and theoretical considerations (Hipp et al., 2011; Rose and Büchel, 2005; Rose et al., 2006; Volberg et al., 2013). To quantify phase coupling between pairs of electrodes we used the imaginary part of coherency, which allows to quantify consistent phase offsets between two signals across trials, while at the same time disregarding phases with zero-offset that are thought to arise form volume conduction (Nolte et al., 2004). Comparing the imaginary part of coherency across the whole electrode-frequency space did not reveal any significant differences either for the low frequencies (cluster-level $p \geq 0.12$, absolute cluster statistic ≤ 290), or for the high frequencies (cluster-level $p \geq 0.077$, absolute cluster statistic ≤ 1221). Importantly, the cluster with the trend towards significance for the high frequencies had a synchronization pattern opposite from that predicted: there was *less* phase coupling in global compared to local conditions.

Phase-coupling source-level results

In addition to the sensor-level phase-coupling we conducted an analogous analysis in the source space. Source-level analysis may be advantageous as it allows reconstruction of local oscillatory activity, which would be intermixed in the scalp data. Therefore, for the frequency bands that are known to play a role in synchrony and in perceptual grouping (theta, beta and low gamma), we also conducted a source-level coherence comparison using the magnitude of coherency as a measure of phase coupling. Specifically we wanted to know if there are brain areas that differentially synchronize with the right posterior parietal cortex in global and local conditions.

We did not find any significant clusters of voxels that differentially synchronized with the right PPC in global and local conditions for either of the four frequency bands tested (all cluster-level $p \geq 0.17$, see also Table 1). An additional region of interest analysis within areas that we expected to be involved in the stimulus processing (parietal cortex, putative V5/MT+ as well as early visual cortex; see methods) revealed that the contralateral, left PPC was significantly stronger phase-coupled with the right PPC in the theta band during the global compared to the local perceptual state ($t = 2.96$, $p = 0.02$ small volume

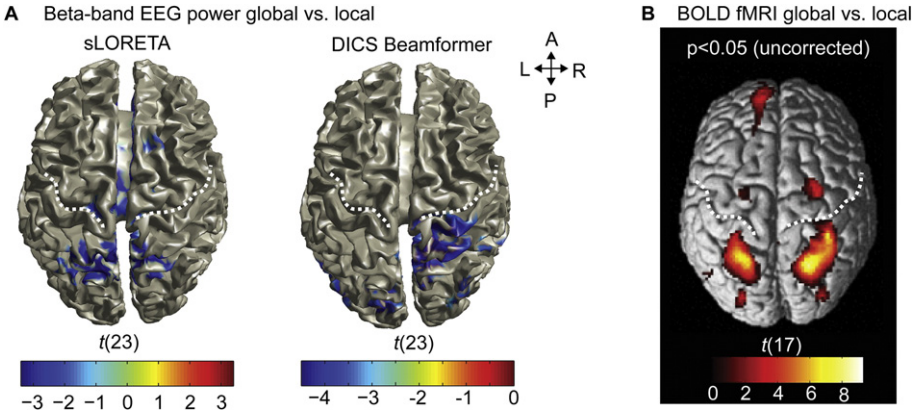

Fig. 4. Source localization of the beta-band power decrease. (A) Localization of beta-band power difference performed using sLORETA (left) and DICS beamformer (right). To illustrate the minima, the results of the t-test using the DICS beamformer were thresholded using a more conservative multiple comparison correction method (absolute maximum statistic). (B) Group results of our previous fMRI experiment (Zaretskaya et al., 2013) replotted here for comparison. Regions that are more active during global compared to local percepts are shown with an uncorrected threshold of $p < 0.05$ for illustration. Dotted white line illustrates the approximate path of the central sulcus.

Table 1
Results of the whole-brain and region of interest source-level phase coupling analysis. The table shows t-values for the statistical comparison of right PPC coupling (coherence) in global and local conditions for different regions of interest in different frequency bands. Whole-brain cluster statistics were computed separately for positive and negative clusters, but the absolute values are reported in the table. P-values for the region of interest analysis are corrected for small volume with radius of 10 mm around the central coordinates. MNI coordinates of the centres of each ROI are given in square brackets. EVC: early visual cortex; ESC: extrastriate cortex; PPC: posterior parietal cortex r: right; l: left.

	theta: 4–7 Hz	alpha: 8 = 12 Hz	beta: 13–24 Hz	Low gamma: 35–45 Hz	High gamma: 55–120 Hz
Whole brain	Stat < = 651 p > = 0.13	Stat < = 12.43 p > = 0.89	Stat < = 14.95 p > = 0.81	Stat < = −64.62 p > = 0.60	Stat < = −141.74 p > = 0.30
EVC [0–100 0]	Stat = 0.7 p = 0.85	Stat = 0.87 p = 0.69	Stat = 0.85 p = 0.65	Stat = −0.96 p = 0.59	Stat = 0.94 p = 0.85
lESC [−50 − 74 00]	Stat = 0.89 p = 0.69	Stat = −0.49 p = 1	Stat = 0.56 p = 0.90	Stat = −0.71 p = 0.76	Stat = −2.03 p = 0.13
rESC [46 − 68 − 2]	Stat = 1.74 p = 0.12	Stat = 1.10 p = 0.47	Stat = −1.35 p = 0.27	Stat = −0.58 p = 0.74	Stat = −1.16 p = 0.48
lPPC [−26 − 56 52]	Stat = 2.96 p = 0.02	Stat = 1.21 p = 0.59	Stat = 1.60 p = 0.31	Stat = −2.31 p = 0.07	Stat = −1.77 p = 0.20
rPPC [28 − 56 54]	Stat = 1.10 p = 0.53	Stat = −1.06 p = 0.82	p = −1.02 p = 0.79	Stat = 0.74 p = 1	Stat = −0.92 p = 0.90

corrected). However, we could not reproduce similar results when doing an equivalent analysis with sLORETA-localized sources (all t < = 0.98). This lack of reproducibility across different source localization techniques, together with the relatively high p-value does not give us enough confidence to rule out a false positive result.

Discussion

Summary

In this study we compared oscillatory brain activity that accompanied the continuous perception as well as the formation of a global illusory Gestalt with that of local elements. We used a bistable stimulus that led to perceptual alternations between local motion of dots and global motion of two illusory squares, while the physical properties of the stimulus remained unchanged. We found a reduction of power in the beta-band before the onset of global percept as well as during continuous global compared to local perception, the latter difference being localized to the posterior parietal cortex using two distinct source localization methods. Our results thus suggest that a decrease in parietal beta-band power underlies perceptual grouping.

Previous findings on oscillatory mechanisms of perceptual grouping

In contrast to theoretical predictions (Fries, 2005) and previous empirical findings (Rose et al., 2006; Tallon-Baudry and Bertrand, 1999; Uhlhaas et al., 2006; Volberg et al., 2013) we did not find any evidence for increased neural phase synchronization during Gestalt perception in our data neither locally nor between remote areas. Several reasons could account for this negative result.

One reason is the possibly insufficient sensitivity of our methods. A source analysis using MEG in combination with individual MRI based head models could have provided us with better prerequisites to detect synchrony, especially in the gamma band. In addition, the observed significant power differences in the beta band could have precluded, at least for the beta-band, the detection of phase-locking differences.

However, it is also possible that the previously reported grouping-related increase in synchronization is transient in nature and absent in sustained neural activity related to perceiving Gestalt. Previous studies measured stimulus-locked activity, containing both *evoked* (phase locked to the stimulus onset) and *induced* (not phase locked to the stimulus onset) response components, within the first second after the stimulus onset (Rose et al., 2006; Uhlhaas et al., 2006; Volberg et al., 2013). The observed synchronization may reflect evoked synchronicity associated with the change in visual input. In contrast to these studies, our experimental design and analysis eliminated any visual phase locking. Our epoch definition depended entirely on subjective reports, was jittered depending on percept duration, excluded the first second after reported percept changes, and focused on mid-epochs of stable percepts that could be seconds away from stimulus onset and percept change. The intrinsic neural activity associated with distinct perceptual states, may thus not be accompanied by changes in long-range phase coupling.

A less popular yet equally rightful hypothesis suggests that a higher-order composite percept may require a more complex neural code representing it. A more complex neural code would require independent activity of a larger number of cortical neurons. This would result in an overall desynchronization of oscillatory activity and a corresponding decrease in band-limited power in scalp recordings, termed "event-related desynchronization" (ERD) (Pfurtscheller and Lopes da Silva, 1999; Pfurtscheller et al., 1994). In visual perception, decrease in power has been systematically observed in lower and mid-range frequency bands during increased processing demands and in particular in the alpha band with attention (Sauseng et al., 2005; Siegel et al., 2008; Thut et al., 2006; Worden et al., 2000; Wyart and Tallon-Baudry, 2008), In our experiment power decrease has been observed specifically in the beta-band, which clearly dissociates it from the above phenomena. However the general mechanisms underlying Gestalt-related desynchronization could be similar.

Beta oscillations as an indicator of subjective perceptual change

Compared to other frequency bands, the functional role of beta oscillations remains controversial and rather vague (Engel and Fries, 2010). Our finding of beta oscillations being involved in internally generated global perception sheds additional light onto its possible role.

In a study examining the relationship between LFP power fluctuations and visual stimulation, beta-band changes, in contrast to higher and lower LFP band, were found to be unrelated to external stimulation (Belitski et al., 2008). The authors concluded that beta oscillations may play a modulatory role rather than being involved in the processing of external stimulation. Indeed, beta-band power modulation has been observed in other experimental paradigms involving constant physical stimulation associated with vivid changes in subjective experience. Purely perceptual (not externally induced) disappearances of a salient visual target were closely reflected in the LFP power of lower frequencies including the beta-band (Maier et al., 2008; Wilke et al., 2006). Alongside gamma power increases (Doesburg et al., 2005; Ehm et al., 2011) and alpha power decreases (Işoğlu-Alkaç and Strüber, 2006; Strüber and Herrmann, 2002), decreases in beta-band power (Okazaki et al., 2008; Piantoni et al., 2010) have also been reported in perceptual transitions during various forms of bistable perception in humans (Kornmeier and Bach, 2012). Notably, the transitions between the two percepts during bistable viewing have also been linked to the parietal cortex (Britz et al., 2009, 2011; Carmel et al., 2010; Kanai et al., 2010,

2011; Zaretskaya et al., 2010). Our results thus fall in line with the idea that beta-band power modulations reflect internal rather than stimulus-induced states of the brain.

Our findings can also be interpreted in terms of the recently proposed "status quo" hypothesis of beta oscillation (Engel and Fries, 2010). Based on evidence from visual, motor and other modalities, the authors propose that beta band oscillatory activity serves to maintain the current default state of the system, which, if disrupted, leads to beta-band power reduction. For our stimulus, local perception is the initial default percept (Anstis and Kim, 2011) that then changes to the global, illusory, percept and then continues to alternate. For the generalized flash suppression paradigm used in the primate studies (Maier et al., 2008; Wilke et al., 2006), the target presence is the initial "default percept", and the beta band decrease accompanies the transition to a non-default state, i.e. its illusory disappearance. In both cases, it is the change from the (non-illusory) default to a (illusory) non-default (alternative) percept that is accompanied by a beta-band decrease.

Consistent with this idea, another EEG study found reduced beta band power during illusory compared to veridical motion direction in the wagon wheel illusion (Piantoni et al., 2010). However, the speculation of the authors of that study that beta-power reflects the likelihood of the percept (with veridical motion being more likely), which was true for their data, appears not to generalize. In our study, the illusory global motion slightly predominated, yet it was still accompanied by a beta-band power decrease. Hence, we propose that beta band activity is more likely to be related to illusoriness of the percept rather than to its likelihood.

Oscillations and BOLD

Global perception was accompanied by beta power decrease in the same regions where we previously observed an increase in the BOLD signal using the same stimulus (Fig. 4B, Zaretskaya et al., 2013). The apparent contradiction between a decrease in band-limited beta power and an increase in BOLD signal is in fact an established relationship between the two signals. It has been reported during both rest and task execution, across different cortical regions (Hanslmayr et al., 2011; Ritter et al., 2009; Yuan et al., 2010). A recent EEG-fMRI study showed that while gamma power correlated positively with BOLD signal, alpha and beta show a negative correlation (Scheeringa et al., 2011). During perception of our stimulus, BOLD signal increase and beta power decrease may thus reflect two aspects of the same neural process.

Parietal cortex links grouping and attention

Two independent source localization approaches identified parietal cortex as the likely location of beta-band power decrease. Parietal cortex in the human brain is associated with visual attention (Corbetta and Shulman, 2002; Kastner and Ungerleider, 2000; Yantis and Serences, 2003). The neural substrates of attention and grouping may therefore be shared, as parietal cortex is active in both. Despite the anatomical similarity, the oscillatory mechanisms may still be different, as the involved frequency bands are clearly distinct: while alpha band is mediating attentional processes (Sauseng et al., 2005; Siegel et al., 2008; Thut et al., 2006; Worden et al., 2000; Wyart and Tallon-Baudry, 2008), our study suggests that parietal beta may be specific to grouping.

Interestingly, a recent study directly linked changes in power of alpha/beta oscillations, but not gamma oscillations, to cholinergic modulation (Bauer et al., 2012). Acetylcholine administration augmented attention-related decreases in alpha and beta power without significantly changing the gamma oscillations. Notably, this decrease was also localized to the PPC. A testable prediction is therefore that global perception is mediated by fluctuations in ACh levels.

In apparent contradiction with our findings, another study did find a modulation of the alpha band power related to perceptual grouping (Flevaris et al., 2013). Using a bistable stimulus of a partially occluded moving diamond the authors observed alpha band power decreases before participants reported a switch towards the global percept, which may be indicative of enhanced attention associated with the global percept. Our additional analysis of peri-switch activity showed a decrease in beta, but no change in alpha power before the onset of the global percept. Further experiments are needed to shed more light onto the nature of this discrepancy in results.

Conclusion

In sum, we have shown that continuous perception of global Gestalt is associated with a decrease in parietal beta-band power. Our results thus point to the importance of beta-band power decrease for spatial binding and Gestalt perception. They also suggest that part of the mechanisms of spatial binding and visual attention are shared, as both involve neural activity of the posterior parietal cortex.

Supplementary data to this article can be found online at http://dx.doi.org/10.1016/j.neuroimage.2015.02.049.

Acknowledgements

The authors would like to thank Didem Korkmaz-Hacialihafiz and Joachim Bellet for help with preparing the electrodes, and Mario Kleiner for help with technical issues. This work was funded by the Centre for Integrative Neuroscience Tübingen through the German Excellence Initiative (EXC307) and the German Research Foundation grant Nr. BA4914/1-1.

References

Aissani, C., Martinerie, J., Yahia-Cherif, L., Paradis, A.-L., Lorenceau, J., 2014. Beta, but not gamma, band oscillations index visual form-motion integration. PLoS One 9, e95541. http://dx.doi.org/10.1371/journal.pone.0095541.

Anstis, S., Kim, J., 2011. Local versus global perception of ambiguous motion displays. J. Vis. 11, 13. http://dx.doi.org/10.1167/11.3.13.

Balint, R., 1909. Seelenlähmung des Schauens, optische Ataxie, raümliche Störung der Aufmerksamkeit. Monatsschr. Psychiatr. Neurol. 25, 51–81.

Bauer, M., Kluge, C., Bach, D., Bradbury, D., Heinze, H.J., Dolan, R.J., Driver, J., 2012. Cholinergic enhancement of visual attention and neural oscillations in the human brain. Curr. Biol. 22, 397–402. http://dx.doi.org/10.1016/j.cub.2012.01.022.

Belitski, A., Gretton, A., Magri, C., Murayama, Y., Montemurro, M.A., Logothetis, N.K., Panzeri, S., 2008. Low-frequency local field potentials and spikes in primary visual cortex convey independent visual information. J. Neurosci. 28, 5696–5709. http://dx.doi.org/10.1523/JNEUROSCI. 0009-08.2008.

Britz, J., Landis, T., Michel, C.M., 2009. Right parietal brain activity precedes perceptual alternation of bistable stimuli. Cereb. Cortex 19, 55–65. http://dx.doi.org/10.1093/cercor/bhn056.

Britz, J., Pitts, M.A., Michel, C.M., 2011. Right parietal brain activity precedes perceptual alternation during binocular rivalry. Hum. Brain Mapp. 32, 1432–1442.

Buzsáki, G., Draguhn, A., 2004. Neuronal oscillations in cortical networks. Science 304, 1926–1929. http://dx.doi.org/10.1126/science.1099745.

Carmel, D., Walsh, V., Lavie, N., Rees, G., 2010. Right parietal TMS shortens dominance durations in binocular rivalry. Curr. Biol. 20, R799–R800. http://dx.doi.org/10.1016/j.cub.2010.07.036.

Corbetta, M., Shulman, G.L., 2002. Control of goal-directed and stimulus-driven attention in the brain. Nat. Rev. Neurosci. 3, 201–215. http://dx.doi.org/10.1038/nrn755.

Doesburg, S.M., Kitajo, K., Ward, L.M., 2005. Increased gamma-band synchrony precedes switching of conscious perceptual objects in binocular rivalry. Neuroreport 16, 1139–1142.

Ehm, W., Bach, M., Kornmeier, J., 2011. Ambiguous figures and binding: EEG frequency modulations during multistable perception. Psychophysiology 48, 547–558. http://dx.doi.org/10.1111/j.1469-8986.2010.01087.x.

Engel, A.K., Fries, P., 2010. Beta-band oscillations – signalling the status quo? Curr. Opin. Neurobiol. 20, 156–165. http://dx.doi.org/10.1016/j.conb.2010.02.015.

Flevaris, A.V., Martínez, A., Hillyard, S.A., 2013. Neural substrates of perceptual integration during bistable object perception. J. Vis. 13, 17. http://dx.doi.org/10.1167/13.13.17.

Fries, P., 2005. A mechanism for cognitive dynamics: neuronal communication through neuronal coherence. Trends Cogn. Sci. 9, 474–480.

Gross, J., Kujala, J., Hamalainen, M., Timmermann, L., Schnitzler, A., Salmelin, R., 2001. Dynamic imaging of coherent sources: Studying neural interactions in the human brain. Proc. Natl. Acad. Sci. U. S. A. 98, 694–699. http://dx.doi.org/10.1073/pnas.98.2.694.

Gross, J., Baillet, S., Barnes, G.R., Henson, R.N., Hillebrand, A., Jensen, O., Jerbi, K., Litvak, V., Maess, B., Oostenveld, R., Parkkonen, L., Taylor, J.R., van Wassenhove, V., Wibral, M., Schoffelen, J.-M., 2013. Good practice for conducting and reporting MEG research. Neuroimage 65, 349–363. http://dx.doi.org/10.1016/j.neuroimage.2012.10.001.

Hanslmayr, S., Volberg, G., Wimber, M., Raabe, M., Greenlee, M.W., Bäuml, K.-H.T., 2011. The relationship between brain oscillations and BOLD signal during memory formation: a combined EEG-fMRI study. J. Neurosci. 31, 15674–15680. http://dx.doi.org/10.1523/JNEUROSCI. 3140-11.2011.

Hanslmayr, S., Volberg, G., Wimber, M., Dalal, S.S., Greenlee, M.W., 2013. Prestimulus oscillatory phase at 7 Hz gates cortical information flow and visual perception. Curr. Biol. 23, 2273–2278. http://dx.doi.org/10.1016/j.cub.2013.09.020.

Hipp, J.F., Engel, A.K., Siegel, M., 2011. Oscillatory synchronization in large-scale cortical networks predicts perception. Neuron 69, 387–396. http://dx.doi.org/10.1016/j.neuron.2010.12.027.

Işoğlu-Alkaç, U., Strüber, D., 2006. Necker cube reversals during long-term EEG recordings: sub-bands of alpha activity. Int. J. Psychophysiol. 59, 179–189. http://dx.doi.org/10.1016/j.ijpsycho.2005.05.002.

Jung, T.P., Makeig, S., Humphries, C., Lee, T.W., McKeown, M.J., Iragui, V., Sejnowski, T.J., 2000. Removing electroencephalographic artifacts by blind source separation. Psychophysiology 37, 163–178.

Kanai, R., Bahrami, B., Rees, G., 2010. Human parietal cortex structure predicts individual differences in perceptual rivalry. Curr. Biol. 20, 1626–1630. http://dx.doi.org/10.1016/j.cub.2010.07.027.

Kanai, R., Carmel, D., Bahrami, B., Rees, G., 2011. Structural and functional fractionation of right superior parietal cortex in bistable perception. Curr. Biol. 21, R106–R107. http://dx.doi.org/10.1016/j.cub.2010.12.009.

Kastner, S., Ungerleider, L.G., 2000. Mechanisms of visual attention in the human cortex. Annu. Rev. Neurosci. 23, 315–341. http://dx.doi.org/10.1146/annurev.neuro.23.1.315.

Keil, J., Müller, N., Hartmann, T., Weisz, N., 2014. Prestimulus beta power and phase synchrony influence the sound-induced flash illusion. Cereb. Cortex 24, 1278–1288. http://dx.doi.org/10.1093/cercor/bhs409.

Kirshner, H.S., Lavin, P.J.M., 2006. Posterior cortical atrophy: a brief review. Curr. Neurol. Neurosci. Rep. 6, 477–480.

Kornmeier, J., Bach, M., 2012. Ambiguous figures – what happens in the brain when perception changes but not the stimulus. Front. Hum. Neurosci. 6, 51. http://dx.doi.org/10.3389/fnhum.2012.00051.

Luria, A.R., 1959. Disorders of "simultaneous perception" in a case of bilateral occipito-parietal brain injury. Brain 82, 437–449.

Maier, A., Wilke, M., Aura, C., Zhu, C., Ye, F.Q., Leopold, D.A., 2008. Divergence of fMRI and neural signals in V1 during perceptual suppression in the awake monkey. Nat. Neurosci. 11, 1193–1200. http://dx.doi.org/10.1038/nn.2173.

Maris, E., Oostenveld, R., 2007. Nonparametric statistical testing of EEG- and MEG-data. J. Neurosci. Methods 164, 177–190.

Nichols, T.E., Holmes, A.P., 2002. Nonparametric permutation tests for functional neuroimaging: a primer with examples. Hum. Brain Mapp. 15, 1–25.

Niedermeyer, E., Lopes da Silva, F.H. (Eds.), 2005. Electroencephalography: basic principles, clinical applications, and related fields. Lippincott Williams & Wilkins, Philadelphia.

Nolte, G., Bai, O., Wheaton, L., Mari, Z., Vorbach, S., Hallett, M., 2004. Identifying true brain interaction from EEG data using the imaginary part of coherency. Clin. Neurophysiol. 115, 2292–2307. http://dx.doi.org/10.1016/j.clinph.2004.04.029.

Okazaki, M., Kaneko, Y., Yumoto, M., Arima, K., 2008. Perceptual change in response to a bistable picture increases neuromagnetic beta-band activities. Neurosci. Res. 61, 319–328. http://dx.doi.org/10.1016/j.neures.2008.03.010.

Olbrich, S., Mulert, C., Karch, S., Trenner, M., Leicht, G., Pogarell, O., Hegerl, U., 2009. EEG-vigilance and BOLD effect during simultaneous EEG/fMRI measurement. Neuroimage 45, 319–332.

Pascual-Marqui, R.D., 2002. Standardized low-resolution brain electromagnetic tomography (sLORETA): technical details. Methods Find. Exp. Clin. Pharmacol. 24 (Suppl. D), 5–12.

Pascual-Marqui, R.D., Esslen, M., Kochi, K., Lehmann, D., 2002. Functional imaging with low-resolution brain electromagnetic tomography (LORETA): a review. Methods Find. Exp. Clin. Pharmacol. 24 (Suppl. C), 91–95.

Pfurtscheller, G., Lopes da Silva, F.H., 1999. Event-related EEG/MEG synchronization and desynchronization: basic principles. Clin. Neurophysiol. 110, 1842–1857.

Pfurtscheller, G., Neuper, C., Mohl, W., 1994. Event-related desynchronization (ERD) during visual processing. Int. J. Psychophysiol. 16, 147–153. http://dx.doi.org/10.1016/0167-8760(89)90041-X.

Piantoni, G., Kline, K.A., Eagleman, D.M., 2010. Beta oscillations correlate with the probability of perceiving rivalrous visual stimuli. J. Vis. 10, 18. http://dx.doi.org/10.1167/10.13.18.

Ritter, P., Moosmann, M., Villringer, A., 2009. Rolandic alpha and beta EEG rhythms' strengths are inversely related to fMRI-BOLD signal in primary somatosensory and motor cortex. Hum. Brain Mapp. 30, 1168–1187. http://dx.doi.org/10.1002/hbm.20585.

Romei, V., Driver, J., Schyns, P.G., Thut, G., 2011. Rhythmic TMS over parietal cortex links distinct brain frequencies to global versus local visual processing. Curr. Biol. 21, 334–337. http://dx.doi.org/10.1016/j.cub.2011.01.035.

Rose, M., Büchel, C., 2005. Neural coupling binds visual tokens to moving stimuli. J. Neurosci. 25, 10101–10104. http://dx.doi.org/10.1523/JNEUROSCI. 2998-05.2005.

Rose, M., Sommer, T., Büchel, C., 2006. Integration of local features to a global percept by neural coupling. Cereb. Cortex 16, 1522–1528. http://dx.doi.org/10.1093/cercor/bhj089.

Sasaki, Y., Hadjikhani, N., Fischl, B., Liu, A.K., Marrett, S., Dale, A.M., Tootell, R.B., Marret, S., 2001. Local and global attention are mapped retinotopically in human occipital cortex. Proc. Natl. Acad. Sci. U. S. A. 98, 2077–2082. http://dx.doi.org/10.1073/pnas.98.4.2077.

Sauseng, P., Klimesch, W., Stadler, W., Schabus, M., Doppelmayr, M., Hanslmayr, S., Gruber, W.R., Birbaumer, N., 2005. A shift of visual spatial attention is selectively associated with human EEG alpha activity. Eur. J. Neurosci. 22, 2917–2926.

Scheeringa, R., Fries, P., Petersson, K.-M., Oostenveld, R., Grothe, I., Norris, D.G., Hagoort, P., Bastiaansen, M.C.M., 2011. Neuronal dynamics underlying high- and low-frequency EEG oscillations contribute independently to the human BOLD signal. Neuron 69, 572–583. http://dx.doi.org/10.1016/j.neuron.2010.11.044.

Siegel, M., Donner, T.H., Oostenveld, R., Fries, P., Engel, A.K., 2008. Neuronal synchronization along the dorsal visual pathway reflects the focus of spatial attention. Neuron 60, 709–719. http://dx.doi.org/10.1016/j.neuron.2008.09.010.

Singer, W., 2007. Binding by synchrony. Scholarpedia 2, 1657. http://dx.doi.org/10.4249/scholarpedia.1657.

Smith, M.L., Gosselin, F., Schyns, P.G., 2006. Perceptual moments of conscious visual experience inferred from oscillatory brain activity. Proc. Natl. Acad. Sci. U. S. A. 103, 5626–5631. http://dx.doi.org/10.1073/pnas.0508972103.

Strüber, D., Herrmann, C.S., 2002. MEG alpha activity decrease reflects destabilization of multistable percepts. Brain Res. Cogn. Brain Res. 14, 370–382.

Strüber, D., Rach, S., Trautmann-Lengsfeld, S.A., Engel, A.K., Herrmann, C.S., 2013. Antiphasic 40 Hz oscillatory current stimulation affects bistable motion perception. Brain Topogr. http://dx.doi.org/10.1007/s10548-013-0294-x.

Tallon-Baudry, C., 2009. The roles of gamma-band oscillatory synchrony in human visual cognition. Front. Biosci. 14, 321–332.

Tallon-Baudry, C., Bertrand, O., 1999. Oscillatory gamma activity in humans and its role in object representation. Trends Cogn. Sci. 3, 151–162.

Tallon-Baudry, C., Bertrand, O., Delpuech, C., Pernier, J., 1996. Stimulus specificity of phase-locked and Non-phase-locked 40 Hz visual responses in human. J. Neurosci. 16, 4240–4249.

Thut, G., Nietzel, A., Brandt, S.A., Pascual-Leone, A., 2006. Alpha-band electroencephalographic activity over occipital cortex indexes visuospatial attention bias and predicts visual target detection. J. Neurosci. 26, 9494–9502. http://dx.doi.org/10.1523/JNEUROSCI. 0875-06.2006.

Uhlhaas, P.J., Linden, D.E.J., Singer, W., Haenschel, C., Lindner, M., Maurer, K., Rodriguez, E., 2006. Dysfunctional long-range coordination of neural activity during Gestalt perception in schizophrenia. J. Neurosci. 26, 8168–8175. http://dx.doi.org/10.1523/JNEUROSCI. 2002-06.2006.

Van Veen, B.D., van Drongelen, W., Yuchtman, M., Suzuki, A., 1997. Localization of brain electrical activity via linearly constrained minimum variance spatial filtering. IEEE Trans. Biomed. Eng. 44, 867–880. http://dx.doi.org/10.1109/10.623056.

Volberg, G., Wutz, A., Greenlee, M.W., 2013. Top-down control in contour grouping. PLoS One 8, e54085. http://dx.doi.org/10.1371/journal.pone.0054085.

Wilke, M., Logothetis, N.K., Leopold, D.A., 2006. Local field potential reflects perceptual suppression in monkey visual cortex. Proc. Natl. Acad. Sci. U. S. A. 103, 17507–17512. http://dx.doi.org/10.1073/pnas.0604673103.

Wolpert, I., 1924. Die Simultanagnosie – Störung der Gesamtauffassung. Z. Gesamte Neurol. Psychiatr. 93, 397–415.

Worden, M.S., Foxe, J.J., Wang, N., Simpson, G.V., 2000. Anticipatory biasing of visuospatial attention indexed by retinotopically specific alpha-band electroencephalography increases over occipital cortex. J. Neurosci. 20, RC63.

Wyart, V., Tallon-Baudry, C., 2008. Neural dissociation between visual awareness and spatial attention. J. Neurosci. 28, 2667–2679. http://dx.doi.org/10.1523/JNEUROSCI.4748-07.2008.

Yantis, S., Serences, J.T., 2003. Cortical mechanisms of space-based and object-based attentional control. Curr. Opin. Neurobiol. 13, 187–193.

Yuan, H., Liu, T., Szarkowski, R., Rios, C., Ashe, J., He, B., 2010. Negative covariation between task-related responses in alpha/beta-band activity and BOLD in human sensorimotor cortex: an EEG and fMRI study of motor imagery and movements. Neuroimage 49, 2596–2606. http://dx.doi.org/10.1016/j.neuroimage.2009.10.028.

Yuval-Greenberg, S., Tomer, O., Keren, A.S., Nelken, I., Deouell, L.Y., 2008. Transient induced gamma-band response in EEG as a manifestation of miniature saccades. Neuron 58, 429–441. http://dx.doi.org/10.1016/j.neuron.2008.03.027.

Zaretskaya, N., Thielscher, A., Logothetis, N.K., Bartels, A., 2010. Disrupting parietal function prolongs dominance durations in binocular rivalry. Curr. Biol. 20, 2106–2111. http://dx.doi.org/10.1016/j.cub.2010.10.046.

Zaretskaya, N., Anstis, S., Bartels, A., 2013. Parietal cortex mediates conscious perception of illusory gestalt. J. Neurosci. 33, 523–531. http://dx.doi.org/10.1523/JNEUROSCI.2905-12.2013.